RESEARCH ARTICLE

Functional robustness and gene pools of a wastewater nitrification reactor: comparison of dispersed and intact biofilms when stressed by low oxygen and low pH

Yuejian Mao[1,2], Lars R. Bakken[3], Liping Zhao[2] & Åsa Frostegård[1]

[1]Department of Chemistry, Biotechnology and Food Science, Norwegian University of Life Sciences, Aas, Norway; [2]Laboratory of Molecular Microbial Ecology and Ecogenomics, College of Life Science and Biotechnology, Shanghai Jiaotong University, Shanghai, China; and [3]Department of Plant and Environmental Sciences, Norwegian University of Life Sciences, Aas, Norway

Correspondence: Yuejian Mao, Laboratory of Molecular Microbial Ecology and Ecogenomics, College of Life Science and Biotechnology, Shanghai Jiaotong University, Dongchuan Road 800, Shanghai 200240, China. Tel.: +86 21 34204878; fax: +86 21 34204878; e-mail: stone-raining@sjtu.edu.cn

Received 11 April 2008; revised 12 May 2008; accepted 14 May 2008.
First published online 8 July 2008.

DOI:10.1111/j.1574-6941.2008.00532.x

Editor: Jan Dirk van Elsas

Keywords
wastewater treatment; nitrification; denitrification; biofilm; *amoA*.

Abstract

The functional robustness of biofilms in a wastewater nitrification reactor, and the gene pools therein, were investigated. *Nitrosomonas* and *Nitrosospira* spp. were present in similar amounts (cloning-sequencing of ammonia-oxidizing bacteria 16S rRNA gene), and their estimated abundance (1.1×10^9 cells g^{-1} carrier material, based on *amoA* gene real-time PCR) was sufficient to explain the observed nitrification rates. The biofilm also had a diverse community of heterotrophic denitrifying bacteria (cloning-sequencing of *nirK*). Anammox 16S rRNA genes were detected, but not archaeal *amoA*. Dispersed biofilms (DB) and intact biofilms (IB) were incubated in gas-tight reactors at different pH levels (4.5 and 5.5 vs. 6.5) while monitoring O_2 depletion and concentrations of NO, N_2O and N_2 in the headspace. Nitrification was severely reduced by suboptimal O_2 concentrations (10–100 μM) and low pH (IB was more acid tolerant than DB), but the N_2O/NO_3^- product ratio of nitrification remained low ($< 10^{-3}$). The NO_2^- concentrations during nitrification were generally 10 times higher in DB than in IB. Transient NO and N_2O accumulation at the onset of denitrification was 10–10^3 times higher in DB than in IB (depending on the pH). The contrasting performance of DB and IB suggests that the biofilm structure, with anoxic/microoxic zones, helps to stabilize functions during anoxic spells and low pH.

Introduction

Removal of nitrogen from wastewater is often accomplished by consecutive oxidation of ammonia to nitrate (aerated nitrification reactor) and reduction of nitrate to molecular nitrogen (anoxic denitrification reactor). The nitrification reactor appears to be the Achilles heel in such systems. Malfunctioning can be caused by oxygen limitation (Satoh *et al.*, 2003; Blackburne *et al.*, 2007), low pH levels (Ma *et al.*, 2006) or toxic compounds (Belser, 1984; Kelly *et al.*, 2004) in the wastewater entering the reactor. Such disturbances not only reduce the nitrification rates, but may also lead to high emissions of NO and N_2O (Kamschreur *et al.*, 2008). Anthropogenic emissions of these gases have a significant impact on atmospheric chemistry as well as the climate; the global warming potential of N_2O is 300 times higher than that of CO_2 (IPCC, 2001).

The biofilms on the carrier materials in wastewater nitrification reactors contain a functionally diverse community of microorganisms, supported by the flux of ammonium and organic material in the wastewater. Thus, in addition to large populations of autotrophic nitrifying bacteria, the biofilms contain high numbers of heterotrophic bacteria. Many of these are denitrifiers that may reduce a significant fraction of the nitrate, probably due to partly anoxic conditions within the biofilms (Satoh *et al.*, 2004). Other groups of organisms may participate in nitrogen transformations, such as ammonium-oxidizing archaea (AOA) (Francis *et al.*, 2005; Leininger *et al.*, 2006; Park *et al.*, 2006) and bacteria capable of anaerobic ammonium oxidation (anammox) (Vandegraaf *et al.*, 1995; Jetten *et al.*, 1998; Strous *et al.*, 1999).

For stable function, the organisms in the nitrification tank must tolerate fluctuating pH, pulses of toxic substances

and varying loads of ammonia and organic material with the wastewater. The latter will result in fluctuating oxygen consumption rates within the biofilm, thus creating zones that are periodically anoxic. Owing to the variable activities of the nitrifiers and denitrifiers, organisms in the biofilms will be exposed to variable concentrations of NO_2^- and NO, the latter being a toxic intermediate produced from the reduction of NO_2^- by denitrification. Thus, the stability of a nitrification reactor is challenged by external factors as well as toxic intermediates of the nitrogen transformations within the biofilm.

The N_2O released by ammonia-oxidizing bacteria (AOB) represents a minor fraction of the oxidized ammonium (Jiang & Bakken, 1999b), but NO and N_2O emission have been found to increase dramatically in response to oxygen limitation due to reduction of NO_2^- (Remde & Conrad, 1990; Kamschreur *et al.*, 2008). Similarly, denitrifying bacteria appear to release more N_2O than N_2 under suboptimal oxygen concentrations (i.e. suboxic rather than anoxic conditions, Otte *et al.*, 1996), and NO may accumulate to apparently toxic levels during rapid transition from oxic to anoxic conditions (Bergaust *et al.*, 2008). Against this background, the biofilm of a nitrification tank is probably a strong emitter of both NO and N_2O, in particular when stressed by fluctuating oxygen concentrations and pH levels.

We investigated the carrier material from a nitrification tank in a municipal wastewater treatment plant that serves the major parts of the Oslo area in Norway. The incoming wastewater is characterized by low alkalinity and low organic matter content. We assumed that the biofilm would harbour active denitrifying as well as nitrifying bacteria (and possibly anammox bacteria and ammonia-oxidizing *Crenarchaea*). Moreover, we hypothesized that a stable function of the nitrification tank depends on biofilm structures being able to moderate rapid variations in environmental parameters. This was tested by comparing the functional robustness of the intact and dispersed biofilms.

We challenged the microbial community with different pH levels and oxic/anoxic conditions to observe how these fluctuations affected the transient accumulation of NO_2^-, NO and N_2O. Experiments with intact biofilms were carried out by incubation of intact carrier material inside specially designed gas-tight reactors with internal circulation of the liquid phase, allowing monitoring of nitrification rates and headspace concentrations of O_2, CO_2, NO and N_2O. We also carried out identical incubation experiments with dispersed biofilms.

We investigated the bacterial community composition of three reactors using primers targeting the 16S rRNA genes of Eubacteria and AOB, the copper-containing nitrite reductase gene (*nirK*), as well as the eubacterial and archaeal genes coding for ammonia oxidation (*amoA*). Copy numbers of the eubacterial *amoA* gene were quantified by real-time PCR, PCR-denaturing gradient gel electrophoresis (PCR-DGGE) was used to fingerprint the composition of the different genes and clone libraries were constructed and sequenced to further characterize AOB, *amoA* and *nirK*.

A general agreement was found between the observed maximum rates of nitrification (at high oxygen concentrations) and the copy numbers of the *amoA* gene per gram of carrier material. A substantial heterotrophic denitrification potential was evident, both functionally (nitrate reduction under anoxic conditions) and genetically (*nirK* clone sequences affiliated with heterotrophic bacteria dominated). The comparison of dispersed and intact biofilms suggested that the architecture of the biofilm helps to stabilize functions during anoxic spells (lower NO and N_2O emissions) and low pH (higher nitrification rates in intact than in dispersed biofilm).

Materials and methods

Description of the nitrification tank

Nitrifying tanks of a municipal sewage wastewater treatment plant in Norway (Vestfjorden Avløpsselskap, Slemmestad), serving the major part of the Oslo area, were investigated. For a more detailed description of the plant, see Sagberg *et al.* (1998). The tanks contain *c.* 350 m^3 upflow biofilters (Degremont BIOFOR) consisting of (lightweight) expanded clay aggregates (Leca) pellets. The pellets are 3–5 mm in diameter, and have a higher density (1.24 g mL^{-1}) than normal Leca. The pellets are coated with a nitrifying biofilm, built up through several years of continuous flow-through of mechanically purified wastewater rich in ammonium (0.5–2; average 1.2 mM), with organic carbon [total organic carbon (TOC) = 35–45 mg L^{-1}] and alkalinity (2.6 meqv L^{-1}). The wastewater is injected at the bottom of the reaction tank filled with Leca particles; aeration is secured by air injection with the incoming water; the average residence time of the water is 12 min; and the normal temperature is 7 °C. As the water flows through the reactor (100–180, average 160 L s^{-1}), *c.* 50% of TOC is removed, 30% by heterotrophic respiration and 20% by assimilation/adsorption (adding to the biofilm, which is partly removed by vigorous backwashing every 14 h to control its thickness). The calculated rate of heterotrophic respiration on the filter material during normal operation is 1–2 μmol CO_2-C g^{-1} carrier material h^{-1} (based on mass balances for TOC). On the average, 90% of the ammonium is oxidized, resulting in a substantial reduction of pH (near-neutral at inlet, 4.7–6.5 at outlet). The estimated oxidation rate of ammonium during a normal operation is 1–3 μmol N g^{-1} Leca h^{-1}.

Sampling of carrier material

Leca carrier material was sampled using a device consisting of a stick (*c.* 8 m) equipped with a small container that can be opened and closed mechanically from the upper end of the stick. This allowed sampling at defined depths. The sampled Leca carrier particles (50–200 g) were poured into 500-mL sterile bottles, which were immediately transported to the laboratory (1 h) and kept at 4 °C for a maximum of 4 h before incubation experiments and DNA extractions. Air entry during transport and storage was secured by not tightening the lids.

Reaction vessels and incubation conditions

The Leca particles were incubated in a robotized incubation system (Molstad *et al.*, 2007) for measuring nitrification rates and gas production. Two types of incubation vessels were used: one in which Leca particles were crushed and biofilms thus dispersed and another one in which the Leca particles were kept intact. For the 'dispersed biofilm treatment', presterilized 120-mL serum flasks containing a Teflon-coated magnetic stirring bar (as described by Molstad *et al.*, 2007) were used. We wanted to compare this with undisrupted biofilms, which are more similar to the normal operation of the nitrification reactor, and, for this, specially designed steel reactors were used (Fig. 1).

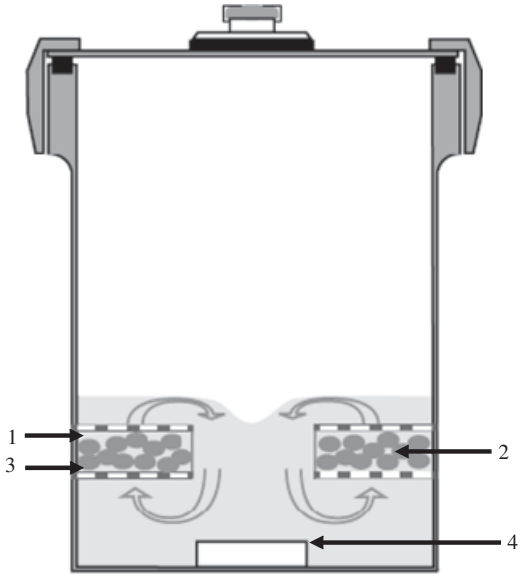

Fig. 1. Gas-tight steel flask, which was designed for intact biofilm incubation. The arrows show continuous up-flow of water through the Leca carrier material and over the edge of the central tube during magnetic stirring. 1, steel screen (1-mm-diameter pores); 2, Leca carrier material with biofilm; 3, nonmagnetic metal screen used for Leca carrier material settlement (1-mm-diameter pores); 4, triangular magnetic stirring bar (25 × 8 mm).

The steel chamber (diameter 4.82 cm; height 7.89 cm) and the gas-tight lid were made of nonmagnetic stainless steel. The total volume of the flask was 145 mL. A rubber ring (6.00 × 5.05 × 0.55 cm) was placed between the chamber top and the screw lid, which ensured minimal leakage of gas (measured air leakage into the helium-filled steel flask was 60 nmol N_2 h^{-1} and 28 nmol O_2 h^{-1}). The lid was equipped with a steel top crimp sealing with the same butyl rubber septa as for the serum flasks. The Leca particles were placed on a steel screen 1.4 cm above the bottom. The screen, which had 1-mm-diameter pores, was equipped with a central tube (2.2 cm diameter, 1.3 cm high). Another screen (also with 1-mm-diameter pores) was placed on top of the Leca particles in order to keep them stable during stirring. Magnetic stirring (Teflon-coated bar at the bottom, 950 r.p.m.) during incubation ensured continuous up-flow of water through the Leca particles and over the edge of the central tube (the minimum liquid to ensure efficient circulation was 55–65 mL). Gas exchange between the liquid phase and the headspace was measured experimentally as described by Molstad *et al.* (2007). The transport coefficient was found to be 4.3×10^{-5} L s^{-1}, which is lower than that for the normal stirring in glass flasks. The reported oxygen concentrations are those calculated for the bulk liquid, using the empirically determined transport coefficient for this particular reactor. The mixing ratio within the bulk water phase was very rapid, as measured by continuous monitoring of electrical conductivity in response to injection of 1 M KCl in between the Leca particles: within 5 s, a stable reading of the electrical conductivity was obtained.

For the 'dispersed biofilm' treatment, 6 g wet weight (ww) of Leca particles were dispersed in 50-mL liquid medium. Stirring resulted in rapid grinding of the pellets into a homogenous, fine-grained slurry within *c.* 1 h, which was assumed to disperse the biofilms effectively. For the 'intact biofilm' treatment, 6 g Leca particles were placed on a screen of presterilized steel reactors, and 65 mL of liquid medium was added. For incubation at a reduced oxygen concentration (to ensure early oxygen depletion), the initial concentration of oxygen in the headspace was adjusted by injecting helium and releasing the overpressure, thus reducing the concentration of both O_2 and N_2 to 1/4 of that in air. During this treatment, the flasks were stirred at 950 r.p.m. to avoid oxygen depletion in the liquid phase. Finally, the medium was supplemented with sterile $(NH_4)_2SO_4$, to reach final NH_4^+ concentrations of 2 or 20 mM. The temperature was maintained at 10 °C during the whole incubation.

Medium

The basic liquid mineral medium contained (in 1 L Milli-Q water) KH_2PO_4, 0.2 g; $CaCl_2 \cdot 2H_2O$, 0.02 g; $MgSO_4 \cdot 7H_2O$, 0.04 g; Fe-NaEDTA, 3.8 mg; $NaMoO_4 \cdot 2H_2O$, 0.1 mg;

$MnCl_2$, 0.2 mg; $CoCl_2 \cdot 6H_2O$, 0.002 mg; $ZnSO_4 \cdot 7H_2O$, 0.1 mg; and $CuSO_4 \cdot 5H_2O$, 0.02 mg (Macdonald & Spokes, 1980; Donaldson & Henderson, 1989). This medium was supplemented with 15 mM 2-(*N*-morpholino)ethanesulphonic acid (MES) buffer and 0.84 mM Na_2CO_3 (Jiang & Bakken, 1999a). The pH was adjusted to three different levels (4.5, 5.5 and 6.5).

Robotized incubation system

The robotized incubation system and tests of performance have been described in detail by Molstad *et al.* (2007). The system allows repeated sampling of headspace gas by piercing the butyl rubber septa of the reaction vessels, and pumping sample gas by a peristaltic pump through the injection loop of a Varian CP 4700 micro gas chromatography (GC for measuring O_2, CO_2, N_2 and N_2O) and further to a Teledyne Instruments chemoluminescence NOx analyser (Model 200A, Advanced Pollution Instrumentation) for measuring NO. By reversing the pump after injection, the sampled gas was replaced by helium, thus avoiding contamination of the headspace by outside air while retaining 1 atm pressure. Despite the high initial N_2 concentration (1/4 of that in air) in the present set-up, we were able to obtain estimates of N_2 production with enough precision to assess the recovery of reduced NO_3^- as N_2.

Sample collection and analysis

Head space gas samples were collected every 2–3 h using the automated sampling system described above. Routines for calculating mass balances based on the known dilution by sampling were used when needed, and the oxygen concentrations in the bulk liquid phase were calculated based on the empirically determined transport coefficient (4.3×10^{-5} L s^{-1} for incubation of an intact biofilm in steel reactors and 28×10^{-5} L s^{-1} for a dispersed biofilm in stirred suspensions). Details of the robotized gas monitoring system and calculation routines were described by Molstad *et al.* (2007) and Bergaust *et al.* (2008).

Liquid samples were collected manually using a 1-mL syringe with a BD Spinal Needle (Becton Dickinson S.A, Madrid Spain, 0.50 × 90 mm). Samples were centrifuged at 10 000 ***g*** for 10 min and stored at −20 °C until analysed for nitrite and nitrate concentrations. Nitrite and nitrate were measured according to ISO 6777-1984 and ISO 7890-3:1988, respectively, using a Tecator FIAstar 5020 analyser (Tecator AB, Höganäs, Sweden).

DNA extraction, PCR amplification, sequencing and sequence analysis

Leca particles were drained and ground to paste using a mortar, and DNA was extracted from a 0.5-g paste using the FastDNA SPIN Kit for Soil (QBiogene, MP Biomedicals, Solon, OH) according to the manufacturer's instructions. The DNA concentration was determined using the NanoDrop ND 1000 Spectrophotometer (NanoDrop Technologies Inc., Wilmington, DE) and was also checked by electrophoresis in 0.8% w/v agarose gels, followed by staining with ethidium bromide (EB).

All the primers used in this study are listed in Table 1. The primers amoA-1F and amoA-2R were used for cloning and quantification of eubacterial *amoA* genes. For *amoA*-DGGE analysis, a GC clamp was added to the 5′-end of amoA-1F (Nicolaisen & Ramsing, 2002). For AOB-DGGE, the V3 region of 16S rRNA gene of the AOB was analysed. A nested amplification was performed (Freitag *et al.*, 2006) in which a larger AOB-specific 16S rRNA gene fragment was first amplified using primers CTO189f and CTO654r, after which a second amplification reaction using primers P2 and P3 was

Table 1. PCR primers used in this study

Targets	Primers	Primer sequences	References
Eubacteria *amoA* gene	amoA-1F*	5′-GGGGTTTCTACTGGTGGT-3′	Rotthauwe *et al.* (1997)
	amoA-2R	5′-CCCCTCKGSAAAGCCTTCTTC-3′	
AOB partial 16S rRNA gene	CTO189fAB†	5′-GGAGRAAAGCAGGGGATCG-3′	Kowalchuk *et al.* (1997)
	CTO189fC†	5′-GGAGGAAAGTAGGGGATCG-3′	
	CTO654r	5′-CTAGCYTTGTAGTTTCAAACGC-3′	
Eubacteria V3 region of	P2	5′-ATTACCGCGGCTGCTGG-3′	Muyzer *et al.* (1993)
16S rRNA gene	P3	GC clamp 5′-CCTACGGGAGGCAGCAG-3′	
Partial *nirK* gene	nirK-1F	5′-GGMATGGTKCCSTGGCA-3′	Braker *et al.* (1998); Geets *et al.* (2007)
	nirK-5R	5′-GCCTCGATCAGRTTRTGG-3′	
Archaeal *amoA* gene	Arch-amoAF	5′-STAATGGTCTGGCTTAGACG-3′	Francis *et al.* (2005)
	Arch-amoAR	5′-GCGGCCATCCATCTGTATGT-3′	
Anammox partial	Pla46rcF	5′- GGATTAGGCATGCAAGTC -3′	Neef *et al.* (1998); Schmid *et al.* (2000)
16S rRNA gene	Amx820R	5′-AAAACCCCTCTACTTAGTGCCC -3′	

*This primer pair was also used for real-time PCR (Hoefel *et al.*, 2005), for *amoA*-DGGE analysis GC clamp was added to the 5′-end of amoA-1F (Nicolaisen & Ramsing, 2002).

†CTO189fAB and CTO189fC were synthesized separately and then mixed 2 : 1 and used as forward primer named CTO189f.

carried out (Table 1). The 25-μL PCR reaction mixture contained 1 U Promega Taq DNA polymerase (Promega Co.), 1 × PCR buffer (Mg^{2+} free), 2 mM $MgCl_2$, 10 pmol of each primer, 200 μM each dNTP and 1 μL template DNA (20 ng). The PCR programs were as described by the respective references (Table 1).

The TOPO TA cloning kit (Invitrogen, Carlsbad) was used to clone the PCR products of *amoA*, *nirK* and the partial 16S rRNA gene of AOB according to the manufacturer's instructions. All PCR products were purified using the QIAquick PCR purification kit (Qiagen, Hilden, Germany) before cloning. Ligations were introduced into chemically competent One Shot *Escherichia coli* DH5α-T1 cells provided by the kit. Clones were randomly selected and used to inoculate in Luria–Bertani (LB) liquid medium (supplemented with 100 μg ampicillin mL^{-1}). Plasmids were extracted from these cultures using the QIAprep Spin Miniprep kit (Qiagen). Those containing the amplified PCR products were sequenced by an ABI PRISM 3700 DNA analyser (Applied Biosystems) using the M13 reverse vector primer and the BigDye™ Terminator sequencing kit (Applied Biosystems).

The 16S rRNA gene sequences obtained were analysed in the RDP database (Cole *et al.*, 2005) using RDP query 2.7 (Dyszynski & Sheldon, 2006), while other sequences were analysed by BLAST_N against the National Center for Biotechnology Information (NCBI) database (http://www.ncbi.nlm.nih.gov/BLAST/). Sequences were aligned by CLUSTAL.X1.81 (Thompson *et al.*, 1997) and phylogenetic trees were constructed by MEGA2 (Kumar *et al.*, 2001) using the unweighted pair group method with the mathematical averages (UPGMA) method. The coverage of the clone library was calculated as $[1 - (n/N)] \times 100$, where n is the number of singletons and N the total number of sequences (Good, 1953).

DGGE

DGGE was carried out in a D-code System apparatus (Bio-Rad Laboratories, Hercules, CA) according to the method described by Muyzer *et al.* (1993). PCR products were run on 7% w/v polyacrylamide gels in 1 × Tris-Acetate-EDTA (TAE) buffer using the denaturing gradient range 25–50% for the V3 region of AOB, 40–58% for *amoA* genes and 32–52% for partial 16S rRNA genes of Eubacteria (100% denaturant corresponds to 7 M urea and 40% deionized formamide). Electrophoresis was carried out at 160 V and 60 °C for 4 h. Gels were stained by SYBR green (Amresco, Solon, OH) for 1 h and then photographed in the Bio-Rad Gel Doc 2000 system (Bio-Rad Laboratories). The migration and intensity of the bands in the DGGE gels were analysed using Quantity One (version 4.4.0, Bio-Rad Laboratories) according to the manufacturer's manual.

Real-time PCR

Eubacterial *amoA* gene copy numbers were determined by real-time PCR using an ABI Prism 7700 Sequence Detector (Applied Biosystems). The primer set (amoA-1F and amoA-2R; Table 1) and the program were as described by Rotthauwe *et al.* (1997) and Hoefel *et al.* (2005). The 25-μL reaction mixture consisted of 2 U Taq DNA polymerase (Promega Co.), 1 × PCR buffer (Mg^{2+} free), 2 mM $MgCl_2$, 10 pmol of each primer, 200 μM of each dNTP, 0.3 μL 10 × SYBR Green (Amresco) and 1 μL template DNA (2 ng). Each sample was measured three times. The amplified products were checked by agarose gel electrophoresis on 1.2% gels.

Data analysis

Before statistical analysis, the band intensity data of DGGE were normalized so that the total intensity of bands in each lane was brought to 100. Principal component analysis (PCA) was performed in MATLAB 7.04 (The Mathworks, Natick, MA) using the program 'PRINCOMP.M'. Similarities between different treatments and the initial material of the Eubacteria, AOB and *amoA* DGGE profiles were analysed by the PAST program (http://folk.uio.no/ohammer/past/) using the Bray–Curtis coefficient (Bray & Curtis, 1957). In Table 2, the columns 'Intact biofilm' and 'Dispersed biofilm' show

Table 2. Bray–Curtis similarity coefficient for DGGE profiles of partial 16S rRNA gene of Eubacteria and AOB, and for the eubacterial *amoA* gene

	Intact biofilm	Dispersed biofilm	2 mM NH_4^+	20 mM NH_4^+	pH 4.5	pH 5.5	PH 6.5
Eubacteria	0.98 ± 0.01	0.94 ± 0.02	0.97 ± 0.02	0.95 ± 0.03	0.97 ± 0.02	0.96 ± 0.03	0.96 ± 0.03
AOB	0.98 ± 0.01	0.92 ± 0.01	0.96 ± 0.03	0.95 ± 0.04	0.96 ± 0.04	0.95 ± 0.04	0.95 ± 0.03
amoA	ND	0.95 ± 0.00	0.94 ± 0.01	0.95 ± 0.00	0.95 ± 0.01	0.94 ± 0.00	0.95 ± 0.00

For each target gene, the DGGE patterns after different treatment incubations were compared with that of the initial material. The columns 'Intact biofilm' and 'Dispersed biofilm' show the average similarity ± SD, including all the different pH and NH_4^+ levels ($n = 6$), when compared with the initial material. The columns 2 and 20 mM NH_4^+ show the average similarity ± SD, including all three pH levels in both intact and dispersed biofilm ($n = 6$), when compared with the initial material. The columns for the three pH levels show the average similarity ± SD, including the two NH_4^+ levels in both intact and dispersed biofilm ($n = 4$), when compared with the initial material. Thus, each column illustrates the main effect of NH_4^+ concentrations and pH levels.

ND, not determined.

the average similarity ± SD, including all the different pH and NH_4^+ levels ($n = 6$), when compared with the initial material. The columns 2 mM NH_4^+ and 20 mM NH_4^+ show the average similarity ± SD, including all three pH levels in both intact and dispersed biofilms ($n = 6$), when compared with the initial material. The columns for the three pH levels show the average similarity ± SD, including the two NH_4^+ levels in both intact and dispersed biofilms ($n = 4$), when compared with the initial material.

Nucleotide sequence accession numbers

The sequences used in this study were deposited in GenBank with accession numbers EU285282–EU285352.

Results

Microbial community fingerprinting

The community composition of Eubacteria and AOB in the biofilms growing on the carrier material in the nitrification tanks was analysed by PCR-DGGE (for primers, see Table 1). Three different nitrification tanks (Nit44, Nit 72 and Nit84) were sampled, all at five different depths (from the bottom to the top: 0, 0.8, 1.6, 2.4 and 3.2 m; the height of the nitrification filter was 4 m). All samples had very similar DGGE patterns (results not shown). In the eubacterial DGGE, only one band differed by being much brighter at 0 m than at the other depths in all three tanks. In the AOB-DGGE, two weak bands were absent in tank Nit44 compared with the other two tanks while the profiles from the different depths were almost the same in all tanks. The similarity indices (Bray–Curtis) for eubacterial communities at different depths in the same tank and in different tanks were higher than 93% and 90%, respectively. For the AOB communities, the values were as high or even higher (98% and 89%, respectively). For all subsequent analyses, samples were taken from the surface material (3.2 m from the bottom) in the Nit72 tank.

DGGE patterns were obtained for Eubacteria, AOB and *amoA* genes from the incubation experiments performed in the laboratory. DGGE fingerprints of the starting material, right after sampling from the nitrification tank, were compared with those obtained from the different treatments at the end of the incubation experiments (supplementary Figs S1–S3). Twenty-nine bands were distinguished in the DGGE fingerprints for Eubacteria (supplementary Fig. S1), covering a wide range of GC/AT ratios. The AOB were represented by 15 bands in the DGGE fingerprint (supplementary Fig. S2) and nine different sequences of the eubacterial *amoA* gene were found (supplementary Fig. S3). The composition of the microbial communities, both total Eubacteria and AOB, was stable and very similar band patterns were seen in the initial material and the material that had been incubated for 120 h (supplementary Figs S1–S3). This visual judgement was confirmed by Bray–Curtis similarity analysis (Table 2), which showed high similarity between the microbial community structure of the starting material (total Eubacteria, AOB or *amoA* genes) and that of the dispersed or intact biofilms in the different treatments at the end of the incubation period, with most of the pairwise comparisons having similarity indices ≥95%. Small and consistent differences were, however, revealed by PCA analysis (Fig. 2a). The first principal component, which explained 73.4% of the variation, separated the intact biofilm from the dispersed biofilm. After 120 h of incubation, the eubacterial community composition in the intact biofilm was similar to that of the starting material, while the composition of the dispersed biofilm changed during the incubation. The PCA

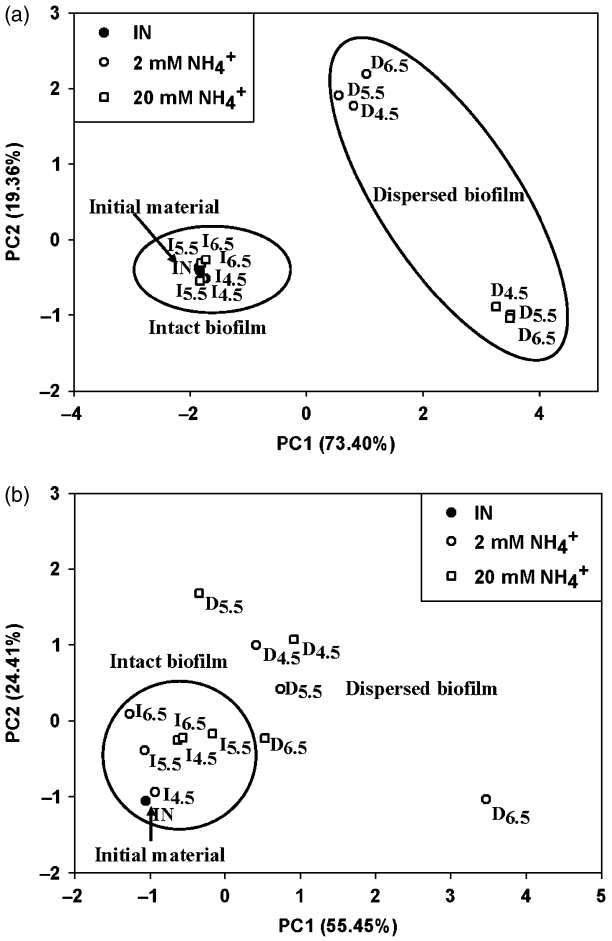

Fig. 2. (a) PCA of the DGGE pattern from the V3 region of the eubacterial 16S rRNA gene; (b) PCA of the DGGE pattern from the V3 region of the AOB 16S rRNA gene. (●) IN, the initial carrier material collected from a nitrification tank of a sewage wastewater treatment (WWTP); (○), 2 mM initial NH_4^+ treatments; (□), 20 mM initial NH_4^+ treatments; D and I, dispersed biofilm and intact biofilm; 4.5, 5.5 and 6.5, three different initial pH levels of the incubations.

also revealed a small effect of the two different NH_4^+ concentrations on the bacteria in the dispersed biofilm, as seen by the separation along PC2. No such separation was seen for the intact biofilm, indicating that the effects of changing environmental conditions were moderated by the protection offered by the biofilm architecture. A similar pattern was seen in the PCA analysis of the AOB-DGGE (Fig. 2b), but in this case there was no difference between the two NH_4^+ levels.

Clone libraries

Clone libraries were constructed for the (partial) 16S rRNA gene of AOB and of anammox, as well as of bacterial *amoA* (ammonia monooxygenase subunit A), archaeal *amoA* and *nirK* (copper-containing nitrite reductase).

In the AOB 16S rRNA gene clone library (Fig. 3), 30 clones were randomly selected for sequencing and 29 sequences were obtained. With a 99% similarity cutoff, these clones were divided into five operation taxonomic units (OTUs) and the clone library coverage was 93.1%. Comparison with the RDP database using RDP query 2.7 showed that the sequences of all clones shared high similarity to those of *Nitrosomonas* or *Nitrosospira* spp. Four of these OTUs, which totally contained 15 clones, were classified into the *Nitrosomonas* group. The largest OTU, which contained 14 clones, was classified into (clustered with) the *Nitrosospira* group.

Anammox were also detected using the primers Planc46f and Amx820R (Neef *et al.*, 1998; Schmid *et al.*, 2000). Sequencing results (Y. Mao *et al.*, unpublished) showed that one OTU, which contained six clones in the anammox clone library, shared 93% similarity to the known anammox bacterium '*Candidatus Brocadia fulgida*' (Schmid *et al.*, 2005).

In the clone library of partial bacterial *amoA* genes (supplementary Fig. S4), 23 sequences were obtained from 30 randomly selected clones. With a 99% similarity cutoff, these clones were divided into six OTUs, and clone library coverage was 91.3%. In the phylogenetic tree, these OTUs were closer to *Nitrosospira* (*briensis*) than to *Nitrosomonas* spp. On analysis of the sequences by BLAST_N against the NCBI database, we found that their closest sequences were bacterial *amoA* gene clones from soil (similarity $> 98\%$).

Attempts were made to clone archaeal *amoA* sequences using primers Arch-amoAF and Arch-amoAR designed by Francis *et al.* (2005). Gel electrophoresis of PCR products showed a band about 100 bp smaller than the expected size (635 bp, Francis *et al.*, 2005). Sequencing showed no similarity to any known archaeal sequences, and not even to any known prokaryotic sequences. It thus seems that these primers captured genes of other origin in this system, and that they should be used with caution. This result also indicates that the abundance of hitherto known AOA was insignificant in this nitrification tank.

Twenty-four clones were randomly selected for the generation of sequences of the nitrite reductase gene *nirK*, and 19 sequences were obtained (Fig. 4). With a 95% similarity cutoff, they were divided into nine OTUs, and clone library coverage was 84.2%. Phylogenetic analysis demonstrated that all *nirK* genes clustered with those of various heterotrophic bacteria (Fig. 4). Most of the OTUs, however, showed low similarity ($< 98\%$) to the genes of known denitrifying strains.

Gas emission analysis

Figure 5 summarizes the gas kinetics during the incubations. Oxygen (μM in liquid, shown as a shaded area) was depleted during the first 30–60 h of incubation, clearly faster in the dispersed than in the intact biofilm treatment. The accumulated oxygen consumption (shown as μmol O_2 per flask) reached somewhat different plateaus depending on the respiration rates. The reason for this is that the oxygen losses due to sampling (replaced by helium; see Molstad *et al.*, 2007) are proportional to the oxygen concentration at each

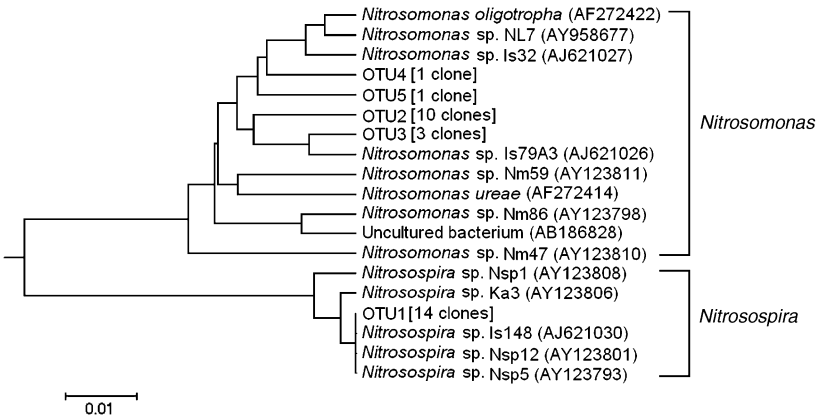

Fig. 3. Phylogenetic analysis of AOB partial 16S rRNA gene of the biofilm from a nitrification tank of a sewage wastewater treatment plant (WWTP). With a similarity cutoff of 99%, 29 AOB clones were divided into five OTUs, clone library coverage 93.1%.

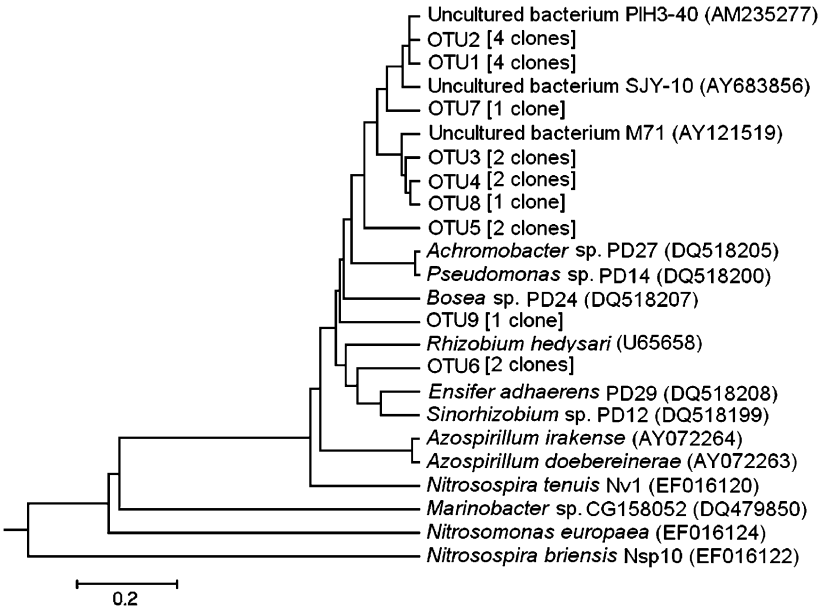

Fig. 4. Phylogenetic analysis of partial copper-containing nitrite reductase (*nirK*) genes of the biofilm from a nitrification tank of a sewage wastewater treatment plant (WWTP). With a similarity cutoff of 95%, 19 *nirK* clones were divided into nine OTUs, clone library coverage 84.2%.

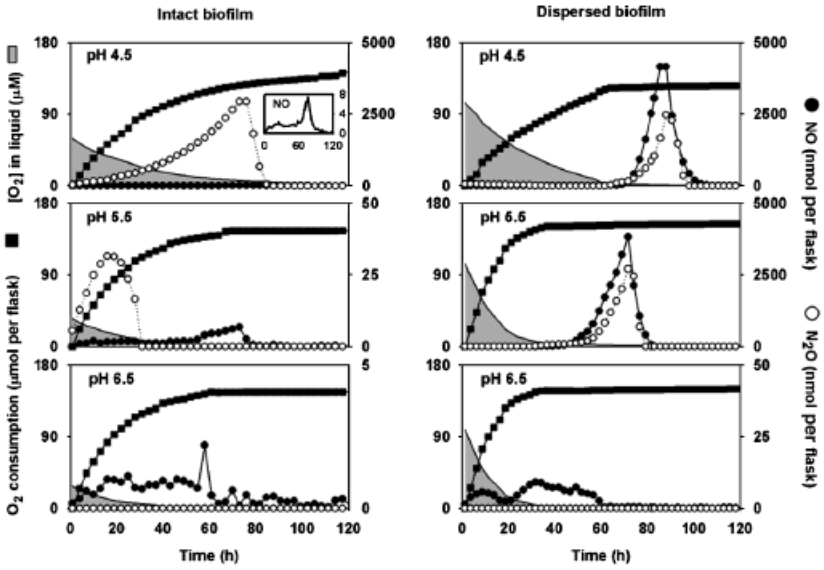

Fig. 5. Gas kinetics of intact and dispersed biofilm treatments, incubated with 20 mM NH_4^+ at three initial pH levels (4.5, 5.5 and 6.5). (–) $[O_2]$, estimated O_2 concentration in the liquid (μM), left *Y*-axis; (■) O_2, total O_2 consumption in each flask (μmol per flask), left *Y*-axis; (●) NO, total amount of NO in each flask (nmol per flask), right *Y*-axis; (○) N_2O, total amount of N_2O in each flask (nmol per flask), right *Y*-axis.

sampling (3.4% per sampling), and thus more oxygen will be removed by sampling from a slowly respiring system than from a rapidly respiring one.

In the dispersed biofilm treatments, high but transient peaks of both NO and N_2O (2500–4000 nmol per flask) appeared after oxygen depletion, but only at the two lowest pH levels (4.5 and 5.5). Incubations with initially higher O_2 levels (21 vol%) showed the same pattern [high transient NO and N_2O peaks after O_2 depletion, but only at the two lowest pH levels (data not shown)]. For all pH treatments, however, a minor accumulation of NO was detected throughout the oxic phase, reaching 2–6 nmol NO per flask (not visible for pH 4.5 and 5.5 in Fig. 5 due to scaling). This aerobic NO accumulation was positively correlated with pH. At the highest pH level, N_2O was not detectable (i.e. below the detection limit, which is 2.5 nmol per flask, Molstad *et al.*, 2007). The absence of detectable N_2O at the highest pH level was confirmed in other incubations (with initial $O_2 = 21$ vol%, 2 and 20 mM NH_4^+, data not shown), but traces of NO were detected throughout the oxic and into the anoxic part of the incubation. These NO levels were 3 orders of magnitude lower than those at the lower pH treatments. In summary, the oxic phase was characterized by a minor accumulation of NO (reaching 2–6 nmol per flask) proportional to the pH level. As the cultures entered the anoxic phase, transient peaks of NO and N_2O (3–4000 nmol per

flask) were observed for the two low pH treatments. Very similar responses to pH were observed for the incubations with 2 mM NH_4^+ (supplementary Fig. S5) as well as other incubations (with initial $O_2 = 21$ vol%, 2 and 20 mM NH_4^+, data not shown). NO is a toxic compound, and its concentration in the liquid is therefore relevant. Assuming equilibrium between headspace and liquid, 1 nmol NO per flask is equivalent to 0.82 nM in the liquid (see Molstad *et al.*, 2007). This implies that NO concentrations in the liquid reached *c.* 3 μM in the dispersed biofilm treatments at the two lowest pH levels, and 100–1000 times lower levels in the intact biofilm treatments at the same pH levels. Much lower concentrations were observed at the highest pH level: 7–8 nM in the dispersed biofilm treatment and around 1 nM in the intact biofilm treatment.

The estimated accumulated N_2 production (results not shown) through the entire incubation period for dispersed biofilms was 10, 20 and 15 μmol N_2 per flask for the pH levels 4.5, 5.5 and 6.6, respectively. The equivalent numbers for the intact biofilms were 6, 10 and 7 μmol N_2 per flask. These values are in reasonable agreement with the peak accumulation of NO_3^- reached during the oxic phase; thus, NO_3^- was largely recovered as N_2.

Nitrification rate and *amoA* gene copy numbers

Figure 6 summarizes the measured NO_2^- and NO_3^- concentrations in the 20 mM NH_4^+ treatments (same treatments as shown in Fig. 5). In the intact biofilm, NO_3^- concentrations reached maximum plateaus long before oxygen depletion, and declined rapidly as the oxygen concentration in the liquid declined below 2–12 μM (compare Figs 5 and 6). In the dispersed biofilm treatment, the NO_3^- concentrations followed similar patterns of accumulation during the oxic phase, and similar rates of decline as oxygen was being depleted. The exception is the dispersed pH 4.5 treatment, in which the rate of oxygen consumption was too low to significantly deplete the oxygen within the time frame of the NO_2^- and NO_3^- measurements. The NO_2^- concentrations fluctuated between 0 and 2 μM (0 and 120 nmol per flask) for the intact biofilm treatments, except for a single peak of 11 μM (660 nmol per flask) at the lowest pH level. In the dispersed biofilm treatment, the measured NO_2^- concentrations reached plateaus at least 1 order of magnitude higher than those in the intact biofilm treatments of pH 5.5 and 6.5 (but not at pH 4.5). In another experiment with 2 mM NH_4^+, the responses to dispersion and pH shown in Figs 5 and 6 were largely reproduced (supplementary Figs S5 and S6).

Table 4 compiles the estimated rates of net nitrification (accumulation of NO_3^- and NO_2^-) and the average oxygen consumption for the first 7 h of incubation (only for the 20 mM NH_4^+ treatment), based on the data presented in Figs 5 and 6. The table allows a more precise comparison of nitrification rates in the different treatments. The maximum rate observed was 3 μmol per flask h^{-1} for a dispersed biofilm at pH 6.5, which is equivalent to 0.5 μmol g^{-1} Leca h^{-1}. In comparison, the nitrification rate during the normal operation of the plant was 1–3 μmol g^{-1} Leca h^{-1}, and similar values were measured in laboratory incubation with full aeration (results not shown).

The nitrification rates responded positively to increasing pH, and more so in the dispersed biofilm than in the intact biofilm treatment. A regression model of respiration as a

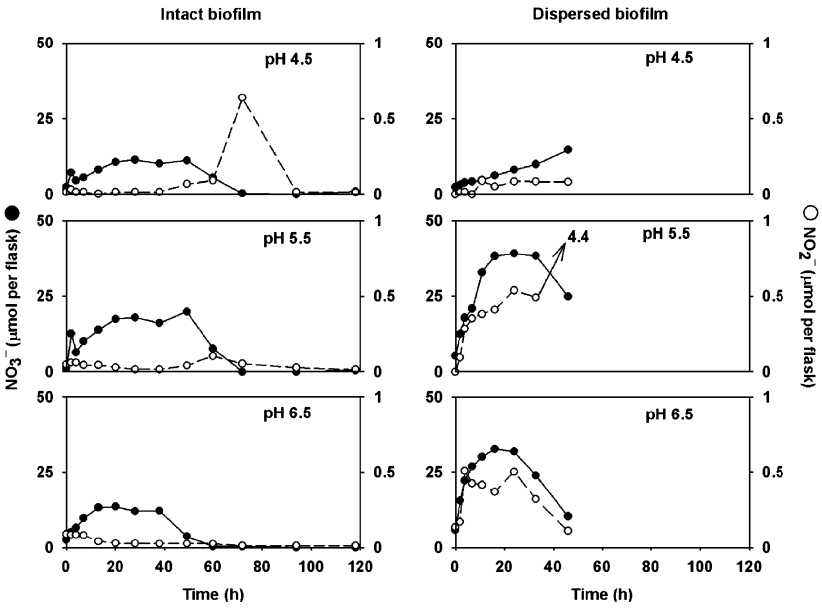

Fig. 6. Total amount of nitrite and nitrate in intact and dispersed biofilm treatments incubated with 20 mM NH_4^+ at three initial pH levels (4.5, 5.5 and 6.5). (●) NO_3^-, total amount of nitrate in the flask (μmol per flask), left *Y*-axis; (○) NO_2^-, total amount of nitrite in the flask (μmol per flask), right *Y*-axis.

function of nitrification based on these data was $R_{esp} = 2.5 + 2.6 \times N_{itr}$, where R_{esp} is the oxygen consumption rate (μmol per flask h^{-1}) and N_{itr} is the nitrification rate in μmol NO_3^- accumulation per flask h^{-1} ($R^2 = 0.93$), which corresponds reasonably well with a basal heterotrophic respiration of 2.5 μmol O_2 per flask h^{-1} and the theoretical oxygen consumption of 2 mol O_2 per mole NO_3^- produced. The calculated N_2O/NO_3^- product ratio was $\leq 10^{-3}$ throughout the early oxic phase of all treatments with pH $\geq$5.5, except the pH = 4.5 treatment of intact biofilm, which had an N_2O/NO_3^- product ratio of 72×10^{-3} (results not shown).

Table 3 shows the estimated numbers of eubacterial *amoA* genes per flask (in samples taken at the end of the incubations). The numbers are based on measured total DNA extracted (Nano-drop), which was 13.5 ± 2.1 μg DNA g^{-1} Leca material, and the number of *amoA* copies per nanogram DNA ($1–2 \times 10^5$ copies ng^{-1} DNA, values for each treatment given in supplementary Table S1; average PCR efficiency 0.96, $R^2 = 0.998$). Assuming that all AOB have the same genome size as *Nitrosomonas europaea*, i.e. 2.8 Mbp = 2.8 fg DNA per cell (Chain *et al.*, 2003), this would imply that DNA from AOB is $0.5–1 \times 10^5 \times 2.8 \times 10^{-15} = 0.14–0.28 \times 10^{-9}$ g ng^{-1} total DNA, i.e. 14–28% of the total gene pool might be derived from AOB.

The estimated numbers of eubacterial *amoA* genes per flask (Table 3) varied too much to allow a precise estimation of treatment effects, but it may be worthwhile to compare the average values with the observed nitrification rates: the gross average number of *amoA* genes (1.29×10^{10} per flask) translates to 6.5×10^9 AOB cells per flask (assuming two copies of *amoA* per genome, and a single genome per cell). The highest observed nitrification rate was 3 μmol NO_3^- per flask h^{-1} (dispersed biofilm, pH 6.5, Table 4), which translates into a specific ammonia oxidation rate per AOB cell of *c.* 0.5 fmol NO_2^- h^{-1}.

Table 3. Abundance of eubacterial *amoA* gene copies in different treatment incubations; 10^{10} copies per flask, ± as the SD; PCR efficiency was 0.96, $R^2 = 0.998$

	Intact biofilm		Dispersed biofilm		
	2 mM NH_4^+	20 mM NH_4^+	2 mM NH_4^+	20 mM NH_4^+	Average
pH 4.5	0.83 ± 0.21	1.60 ± 0.88	0.95 ± 0.32	1.76 ± 0.54	1.29 ± 0.63
pH 5.5	0.91 ± 0.31	0.94 ± 0.06	0.91 ± 0.21	2.04 ± 0.87	1.20 ± 0.65
pH 6.5	1.08 ± 0.96	1.10 ± 0.29	1.56 ± 0.37	1.81 ± 0.98	1.56 ± 0.69

Discussion

The nitrification tanks harboured a large diversity of prokaryotes, which, as expected, consisted of both AOB and heterotrophic bacteria. The DGGE profiles from three large-scale nitrification tanks showed that the microbial communities were surprisingly similar in all tanks at all depths. For the AOB, which are slow-growing and presumably live in protected parts of the biofilms, a spatially and temporally stable community structure can be expected. The results, however, also indicate a high stability of the heterotrophic bacterial community. This is surprising, taking into account that backwashing takes place every 14 h, and thereby a substantial portion of the outer layers of the biofilms, which are presumably largely occupied by heterotrophic bacteria, will regularly be removed.

Cloning-sequencing of AOB-specific 16S rRNA genes revealed a roughly equal distribution between the genera *Nitrosomonas* and *Nitrosospira* and also indicated a higher diversity of *Nitrosomonas* (four OTUs) than of *Nitrosospira* types (one OTU). The numbers of AOB, as calculated from the *amoA* gene copy numbers, were 1.1×10^9 cells g^{-1} Leca, which may comprise up to 30% of the total bacteria. This high percentage appears unrealistic at first glance: The calculated energy flux through AOB during a normal operation would be $<$10% of the energy flux through heterotrophic bacteria (measured heterotrophic respiration is 1–2 μmol CO_2 g^{-1} h^{-1} and measured ammonia oxidation rates are 1–3 μmol NH_3 g^{-1} h^{-1}). However, the frequent backwashing is probably introducing a bias because it can be expected that this operation removes a high fraction of the heterotrophic bacteria and only a small fraction of AOB.

The estimated numbers of AOB were sufficiently high to account for the observed maximum nitrification rates (1–3 μmol NH_3 g^{-1} Leca h^{-1} under a normal operation and in incubations at full aeration; see Table 4). Specific ammonia oxidation rates in cultured strains of *Nitrosospira* were found to be 4.3–7.1 fmol NH_3 $cell^{-1}$ h^{-1} at room

Table 4. Nitrification rate, respiration rate and O_2 levels in different pH treatments, all with 20 mM NH_4^+

	Nitrification rate* (μmol per flask h^{-1})		[O_2]† in liquid (μM)		Respiration rate (μmol per flask h^{-1})	
	Intact biofilm	Dispersed biofilm	Intact Biofilm	Dispersed biofilm	Intact biofilm	Dispersed biofilm
pH 4.5	0.44	0.24	60.1–45.8	104.4–84.2	2.12	3.92
pH 5.5	1.29	2.27	35.0–24.9	103.2–65.5	5.32	9.00
pH 6.5	1.01	3.04	28.4–18.5	99.0–57.8	6.10	9.96

*Nitrification rate: average nitrification rate during the first 7 h incubation.

†[O_2]: estimated O_2 concentration range in the liquid during the first 7 h incubation based on the transport coefficient 4.3×10^{-5} L s^{-1} for intact biofilm and 2.8×10^{-4} L s^{-1} for dispersed biofilm.

temperature (Jiang & Bakken, 1999a), which translates to *c.* 1.5–2.5 fmol NH_3 $cell^{-1}$ h^{-1} at the present incubation temperature (10 °C). Thus, the 1.1×10^9 cells g^{-1} Leca would be able to sustain an activity of 1.6–2.8 μmol NH_3 g^{-1} Leca h^{-1}, which is practically equivalent to the range observed.

The relationship between nitrification rates during a normal operation and the estimated number of ammonia-oxidizing bacterial cells suggests a relatively long turnover time. The rate of ammonia oxidation (1–3 μmol g^{-1} Leca h^{-1}) could support a net growth rate of $1–9 \times 10^6$ *Nitrosospira* g^{-1} Leca, assuming a growth yield of 1–3 cells $pmol^{-1}$ (Jiang & Bakken, 1999a). This translates to a net growth rate of 0.1–1% h^{-1} for the total population, which means that the average residence time of ammonia-oxidizing cells is within a range of 4–40 days. This would support our assumption that the frequent backwashing (every 14 h) probably removes only a minor fraction of the AOB population. In conclusion, the quantified *amoA* gene copy numbers are realistic in relation to the energy flux through ammonia oxidation and thus sufficient to account for the observed nitrification rates.

We were unable to detect AOA by cloning-sequencing. The primers used captured other sequences, of nonprokaryotic origin, in this environment. This does not prove the absence of AOAs, but strongly suggests that these were of little significance in the nitrification tank. This conclusion is further strengthened by the fact that the copy numbers of eubacterial *amoA* were sufficient to account for the observed nitrification rates.

Anammox bacteria were found to be present, as evidenced by cloning-sequencing, but their actual numbers were not quantified. Mass balances and gas measurement do not suggest that anammox metabolism was quantitatively important during a normal operation. However, they may have been active during the anoxic phase of our incubations of intact biofilms. The inner part of the biofilm of the nitrification reactor could provide a suitable environment for anammox for several reasons. One factor is the substrate availability (NO_2^- from AOB, NH_4^+ from water); another favourable factor would be the low load of organic carbon. In fact, the loading of organic carbon would be insufficient to sustain a coupled nitrification–denitrification of the entire ammonium load. With anammox, however, this could possibly be achieved. If so, it would require careful control of the oxygen concentration at moderate levels, plus possibly the regulation of pH to a value around 8, which is the optimum for known anammox bacteria (Jetten *et al.*, 1998; Egli *et al.*, 2001).

The levels of pH and O_2 in the present studies were deliberately chosen to cover not only ranges generally measured in the wastewater treatment plants but also lower levels to mimic possible extreme events. The results showed that the rates of nitrification per gram Leca material for the treatments with 5% O_2 in headspace were ≤ 0.5 μmol g^{-1} Leca h^{-1}. This is $< 50\%$ of the rates measured under a normal operation of the wastewater plant (as well as those observed under full aeration in the laboratory incubation system used in the present investigation). We expected that severe oxygen limitation would result in high N_2O/NO_3^- product ratios for nitrification, but this was generally not the case. The N_2O/NO_3^- product ratios throughout the oxic phase of all treatments with pH ≥ 5.5 were equal to or below the average ratios of $1–2 \times 10^{-3}$ observed in *Nitrosospira* cultures under optimal culturing conditions (Jiang & Bakken, 1999b). The only exception is the pH = 4.5 treatment of intact biofilm, which had an N_2O/NO_3^- product ratio of 72×10^{-3}. Thus, only under extreme conditions (pH 4.5 and low oxygen availability) does nitrification produce N_2O at any significant rate. This result was not expected based on observations of cultures of AOB (Remde & Conrad, 1990; Otte *et al.*, 1996). It is not impossible that the presence of heterotrophic denitrifying bacteria in the biofilm may represents an efficient scavenger of the NO and N_2O produced by AOB. This would explain the low levels of NO and N_2O in the intact biofilm treatments at pH ≥ 5.5, but not those in the oxic phase of the dispersed biofilm. The result appears to be yet another indication that the role of AOB as a source of N_2O emission has been exaggerated in the past (Morkved *et al.*, 2007).

The comparison of nitrification rates and gas kinetics in dispersed vs. intact biofilm treatments strongly suggests that the biofilm includes micro-oxic or even anoxic microsites: the intact biofilm produced detectable N_2O before oxygen depletion (at pH ≤ 5.5), and this phenomenon was eliminated by dispersion (Fig. 5). The most likely explanation for this is that the dispersion ensures efficient exposure of the entire microbial community to the bulk O_2 concentration. Comparison of nitrification rates for the different treatments for the highest pH level suggests that nitrification in the biofilm was severely restricted by oxygen: at pH ≥ 5.5, the dispersed biofilm had much higher nitrification rates than the intact one (Fig. 6 and Table 4). At pH = 4.5, however, the low nitrification rates were clearly higher in the intact biofilm than in the dispersed one. This could reflect some buffering capacity of the biofilm, protecting nitrifying bacteria from the detrimental effect of low pH.

The responses of the organisms in the different treatments as they proceeded into the anoxic phase indicate another evidence that dispersion exposed the entire community to a higher O_2 concentration than they experienced in the biofilm: The dispersed biofilms showed no indications of denitrification before depletion of bulk O_2, whereas the onset of denitrification appears to be gradual in the intact biofilm (Fig. 6). As the dispersed biofilm treatments entered the anoxic state, there was a strongly pH-dependent, transient accumulation of both NO and N_2O. This shows that

the heterotrophic community was able to perform a balanced transition from aerobic respiration to denitrification (i.e. without accumulation of NO and N_2O), but only at near-neutral pH. The intact biofilm, on the other hand, was able to perform a balanced transition (with minimal NO and N_2O levels) even at pH 5.5. The most likely explanation is that the biofilm provides significant buffering against low pH in the water, and this is further strengthened as soon as denitrification is initiated in the biofilm.

A striking performance of the intact biofilm is that the measured accumulation of NO_2^- and NO during transition from oxic to anoxic metabolism was generally 1–2 orders lower than that observed in the dispersed biofilm treatments (Figs 5 and 6; supplementary Figs S5 and S6). It is tempting to speculate why the intact biofilm emits so little NO_2^- and NO. The most likely explanation lies in the role of NO_2^- and NO as strong inducers of denitrification expression, even under micro-oxic conditions (Bergaust *et al.*, 2008). If emitted from anoxic microsites within the biofilm, NO_2^- and NO would enhance denitrification in adjacent fractions of the biofilm, thus representing a strong positive feedback loop in the onset of denitrification. This positive feedback would be much weaker in the dispersed biofilm treatment due to efficient dilution within the bulk liquid. Cells within the biofilm may thus have experienced similar NO_2^- and NO concentrations as the high levels measured in the dispersed biofilm treatments, but with low emissions into the surroundings due to the early onset of efficient denitrification throughout the biofilm. This interpretation underscores the role of an intact biofilm architecture for robustness of the function of a nitrification reactor.

Acknowledgements

This project was supported by the Research Council of Norway (175046/D15/lk) and Vestfjorden Avløpsselskap (VEAS), Slemmestad, Norway. The authors thank Paul Sagberg (VEAS) for information and fruitful discussions and Ola Hilmarsen (Norwegian University of Life Sciences) for constructing the steel reaction vessels.

References

Belser LW (1984) Bicarbonate uptake by nitrifiers: effects of growth rate, pH, substrate concentration, and metabolic inhibitors. *Appl Environ Microbiol* **48**: 1100–1104.

Bergaust L, Shapleigh J, Frostegard A & Bakken L (2008) Transcription and activities of NO(x) reductases in *Agrobacterium tumefaciens*: the influence of nitrate, nitrite and oxygen availability. *Environ Microbiol* DOI: 10.1111/j.1462-2920.2007.01557.x.

Blackburne R, Yuan Z & Keller J (2007) Partial nitrification to nitrite using low dissolved oxygen concentration as the main selection factor. *Biodegradation* **19**: 303–312.

Braker G, Fesefeldt A & Witzel KP (1998) Development of PCR primer systems for amplification of nitrite reductase genes (*nirK* and *nirS*) to detect denitrifying bacteria in environmental samples. *Appl Environ Microbiol* **64**: 3769–3775.

Bray JR & Curtis JT (1957) An ordination of the upland forest communities of southern Wisconsin. *Ecol Monogr* **27**: 326–349.

Chain P, Lamerdin J, Larimer F *et al.* (2003) Complete genome sequence of the ammonia-oxidizing bacterium and obligate chemolithoautotroph *Nitrosomonas europaea*. *J Bacteriol* **185**: 6496–6496.

Cole JR, Chai B, Farris RJ *et al.* (2005) The Ribosomal Database Project (RDP-II): sequences and tools for high-throughput rRNA analysis. *Nucleic Acids Res* **33**: D294–D296.

Donaldson JM & Henderson GS (1989) A dilute medium to determine population-size of ammonium oxidizers in forest soils. *Soil Sci Soc Am J* **53**: 1608–1611.

Dyszynski G & Sheldon WM (2006) RDPquery: A Java program from the Sapelo Program Microbial Observatory for automatic classification of bacterial 16S rRNA sequences based on Ribosomal Database Project taxonomy and Smith–Waterman alignment. (http://www.simo.marsci.uga.edu/public_db/rdp_query.htm).

Egli K, Fanger U, Alvarez PJ, Siegrist H, van der Meer JR & Zehnder AJ (2001) Enrichment and characterization of an anammox bacterium from a rotating biological contactor treating ammonium-rich leachate. *Arch Microbiol* **175**: 198–207.

Francis CA, Roberts KJ, Beman JM, Santoro AE & Oakley BB (2005) Ubiquity and diversity of ammonia-oxidizing archaea in water columns and sediments of the ocean. *Proc Natl Acad Sci USA* **102**: 14683–14688.

Freitag TE, Chang L & Prosser JI (2006) Changes in the community structure and activity of betaproteobacterial ammonia-oxidizing sediment bacteria along a freshwater-marine gradient. *Environ Microbiol* **8**: 684–696.

Geets J, de Cooman M, Wittebolle L *et al.* (2007) Real-time PCR assay for the simultaneous quantification of nitrifying and denitrifying bacteria in activated sludge. *Appl Microbiol Biotechnol* **75**: 211–221.

Good IJ (1953) The population frequencies of species and the estimation of population parameters. *Biometrika* **40**: 237–264.

Hoefel D, Monis PT, Grooby WL, Andrews S & Saint CP (2005) Culture-independent techniques for rapid detection of bacteria associated with loss of chloramine residual in a drinking water system. *Appl Environ Microbiol* **71**: 6479–6488.

IPCC (2001) *Climate Change 2001: The Scientific Basis*. Cambridge University Press, Cambridge, MA.

Jetten MS, Strous M, van de Pas-Schoonen KT *et al.* (1998) The anaerobic oxidation of ammonium. *FEMS Microbiol Rev* **22**: 421–437.

Jiang QQ & Bakken LR (1999a) Comparison of *Nitrosospira* strains isolated from terrestrial environments. *FEMS Microbiol Ecol* **30**: 171–186.

Jiang QQ & Bakken LR (1999b) Nitrous oxide production and methane oxidation by different ammonia-oxidizing bacteria. *Appl Environ Microbiol* **65**: 2679–2684.

Kamschreur MJ, Tan NCG, Kleerebezem R, Picieanu C, Jetten MSM & Loosdrecht MCM (2008) Effect of dynamic process conditions on nitrous oxides emissions from a nitrifying culture. *Environ Sci Technol* **42**: 429–435.

Kelly RT, Henriques ID & Love NG (2004) Chemical inhibition of nitrification in activated sludge. *Biotechnol Bioeng* **85**: 683–694.

Kowalchuk GA, Stephen JR, De Boer W, Prosser JI, Embley TM & Woldendorp JW (1997) Analysis of ammonia-oxidizing bacteria of the beta subdivision of the class Proteobacteria in coastal sand dunes by denaturing gradient gel electrophoresis and sequencing of PCR-amplified 16S ribosomal DNA fragments. *Appl Environ Microbiol* **63**: 1489–1497.

Kumar S, Tamura K, Jakobsen IB & Nei M (2001) MEGA2: molecular evolutionary genetics analysis software. *Bioinformatics* **17**: 1244–1245.

Leininger S, Urich T, Schloter M *et al.* (2006) Archaea predominate among ammonia-oxidizing prokaryotes in soils. *Nature* **442**: 806–809.

Ma Y, Peng Y, Yuan Z, Wang S & Wu X (2006) Feasibility of controlling nitrification in predenitrification plants using DO, pH and ORP sensors. *Water Sci Technol* **53**: 235–243.

Macdonald RM & Spokes JR (1980) A selective and diagnostic medium for ammonia oxidizing bacteria. *FEMS Microbiol Lett* **8**: 143–145.

Molstad L, Dorsch P & Bakken LR (2007) Robotized incubation system for monitoring gases (O(2), NO, N(2)O N(2)) in denitrifying cultures. *J Microbiol Methods* **71**: 202–211.

Morkved PT, Dorsch P & Bakken LR (2007) The N_2O product ratio of nitrification and its dependence on long-term changes in soil pH. *Soil Biol Biochem* **39**: 2048–2057.

Muyzer G, de Waal EC & Uitterlinden AG (1993) Profiling of complex microbial populations by denaturing gradient gel electrophoresis analysis of polymerase chain reaction-amplified genes coding for 16S rRNA. *Appl Environ Microbiol* **59**: 695–700.

Neef A, Amann R, Schlesner H & Schleifer KH (1998) Monitoring a widespread bacterial group: *in situ* detection of planctomycetes with 16S rRNA-targeted probes. *Microbiology* **144**: 3257–3266.

Nicolaisen MH & Ramsing NB (2002) Denaturing gradient gel electrophoresis (DGGE) approaches to study the diversity of ammonia-oxidizing bacteria. *J Microbiol Methods* **50**: 189–203.

Otte S, Grobben NG, Robertson LA, Jetten MSM & Kuenen JG (1996) Nitrous oxide production by *Alcaligenes faecalis* under transient and dynamic aerobic and anaerobic conditions. *Appl Environ Microbiol* **62**: 2421–2426.

Park HD, Wells GF, Bae H, Criddle CS & Francis CA (2006) Occurrence of ammonia-oxidizing archaea in wastewater treatment plant bioreactors. *Appl Environ Microbiol* **72**: 5643–5647.

Remde A & Conrad R (1990) Production of nitricoxide in *Nitrosomonas europaea* by reduction of nitrite. *Arch Microbiol* **154**: 187–191.

Rotthauwe JH, Witzel KP & Liesack W (1997) The ammonia monooxygenase structural gene *amoA* as a functional marker: molecular fine-scale analysis of natural ammonia-oxidizing populations. *Appl Environ Microbiol* **63**: 4704–4712.

Sagberg P, Ryrfors P & Grundnes Berg K (1998) Mass balance in a compact nitrogen and phosphorus WWTP. *Chemical Water and Waste Water Treatment* (Hahn HH, Hoffmann E & Ødegaard H, eds), pp. 231–242. Springer-Verlag, Berlin.

Satoh H, Nakamura Y, Ono H & Okabe S (2003) Effect of oxygen concentration on nitrification and denitrification in single activated sludge flocs. *Biotechnol Bioeng* **83**: 604–607.

Satoh H, Ono H, Rulin B, Kamo J, Okabe S & Fukushi K (2004) Macroscale and microscale analyses of nitrification and denitrification in biofilms attached on membrane aerated biofilm reactors. *Water Res* **38**: 1633–1641.

Schmid M, Twachtmann U, Klein M *et al.* (2000) Molecular evidence for genus level diversity of bacteria capable of catalyzing anaerobic ammonium oxidation. *Syst Appl Microbiol* **23**: 93–106.

Schmid MC, Maas B, Dapena A *et al.* (2005) Biomarkers for *in situ* detection of anaerobic ammonium-oxidizing (anammox) bacteria. *Appl Environ Microbiol* **71**: 1677–1684.

Strous M, Fuerst JA, Kramer EHM *et al.* (1999) Missing lithotroph identified as new planctomycete. *Nature* **400**: 446–449.

Thompson JD, Gibson TJ, Plewniak F, Jeanmougin F & Higgins DG (1997) The CLUSTAL_X windows interface: flexible strategies for multiple sequence alignment aided by quality analysis tools. *Nucleic Acids Res* **25**: 4876–4882.

Vandegraaf AA, Mulder A, Debruijn P, Jetten MSM, Robertson LA & Kuenen JG (1995) Anaerobic oxidation of ammonium is a biologically mediated process. *Appl Environ Microbiol* **61**: 1246–1251.

Supplementary material

The following supplementary material for this article is available online:

Fig. S1. DGGE comparison of the eubacteria communities of different treatment incubations.

Fig. S2. DGGE analysis of V3 regions of 16S rRNA gene of ammonia-oxidizing bacteria (AOB) in different treatment incubations.

Fig. S3. DGGE comparison of *amoA* genes of different treatment incubations.

Fig. S4. Phylogenetic analysis of partial *amoA* genes of the biofilm from a nitrification tank of sewage wastewater treatment plant (WWTP).

Fig. S5. Gas kinetics of intact and dispersed biofilm treatments, incubated with 2 mM NH_4^+ at three initial pH levels (4.5, 5.5 and 6.5).

Fig. S6. Total amount of nitrite and nitrate in intact and dispersed biofilm treatments incubated with 2 mM NH_4^+ at three initial pH levels (4.5, 5.5 and 6.5).

Table S1. Abundance of *amoA* gene in different treatment incubations, 10^5 copies ng^{-1} DNA; PCR efficiency 0.96, $R^2 = 0.998$.

This material is available as part of the online article from: http://www.blackwell-synergy.com/doi/abs/10.1111/j.1574-6941.2008.00532.x

(This link will take you to the article abstract.)

Please note: Blackwell Publishing is not responsible for the content or functionality of any supplementary materials supplied by the authors. Any queries (other than missing material) should be directed to the corresponding author for the article.